Biosensors and Bioelectronics 99 (2018) 312–317

Contents lists available at ScienceDirect

Biosensors and Bioelectronics

journal homepage: www.elsevier.com/locate/bios

Lipopolysaccharides detection on a grating-coupled surface plasmon resonance smartphone biosensor

Jinling Zhang[a,b], Imran Khan[d], Qingwen Zhang[b,c], Xiaohu Liu[a], Jakub Dostalek[d], Bo Liedberg[a,*], Yi Wang[b,c,**]

[a] School of Materials Science and Engineering, Centre for Biomimetic Sensor Science, Nanyang Technological University, 50 Nanyang Avenue, 637553, Singapore
[b] School of Ophthalmology & Optometry, Eye Hospital, School of Biomedical Engineering, Wenzhou Medical University, Wenzhou 325001, PR China
[c] Wenzhou Institute of Biomaterials and Engineering, Chinese Academy of Sciences, Wenzhou 325001, PR China
[d] AIT-Austrian Institute of Technology GmbH, Biosensor Technologies, Muthgasse 11/2, 1190 Vienna, Austria

ARTICLE INFO

Keywords:
Surface plasmon resonance
Biosensor
Smartphone
Synthetic peptide receptor
Lipopolysaccharides

ABSTRACT

We report a smartphone label-free biosensor platform based on grating-coupled surface plasmon resonance (GC-SPR). The sensor system relies on the smartphone's built-in flash light source and camera, a disposable sensor chip with Au diffraction grating and a compact disk (CD) as the spectra dispersive unit. The Au grating sensor chip was modified with a synthetic peptide receptor and employed on the GC-SPR detection of lipopolysaccharides (known as endotoxins) with detection limit of 32.5 ng/mL in water. Upon incubation of various small and macro-molecules with the synthetic peptide modified sensor chips, we concluded the good selectivity of the sensor for LPS detection. In addition, the sensor shows feasibility for the detection of LPS in commonly used clinical injectable fluids, such as clinical-grade 0.9% sodium chloride intravenous infusion, compound sodium lactate intravenous infusion and insulin aspart. The developed sensor platform offers the advantage of portability and simplicity, which is attractive for point-of-care and remote detection of biomedical and environmental targets.

1. Introduction

Rapid on-site detection of chemical and biological species is intensively pursued in the field of early diagnosis, domestic healthcare, and environmental monitoring in remote locations where conventional analytical tools are not available (Hay Burgess et al., 2006; Mudanyali et al., 2012). Conventional analysis in a clinical setting usually requires highly-trained personnel, sophisticated instruments and complex procedures, which may include examinations (X-ray, tomographic and ultrasonic imaging, *etc.*) as well as lab-tests (mass spectroscopy, electrochemical assay and enzyme-linked immunosorbent assay [ELISA] *etc.*) (Mudanyali et al., 2012). These methods provide high sensitivity and accuracy and have definitely advanced modern diagnostics in the developed countries. However, they are not suitable for on-site analysis as they are time consuming, not usable for daily life, and often not affordable for deploying in resource-limited areas.

Multiple strategies have been proposed to address the technical challenges in the area of point-of-care (POC) and field diagnosis based on optical/electrical components (Lim et al., 2009; Potyrailo et al., 2012; Rakow and Suslick, 2000; Shen et al., 2012; Zhu et al., 2011). Other POC systems such as paper-based devices for HIV detection (Wang et al., 2010a) and colorimetric immunoassays (Wang et al., 2010b) have been proposed. Although these simple colorimetric assays can be read by the naked eye, more sensitive and precise analysis require amplification, image capturing and data processing. Among the external auxiliary tools, the smartphones are gradually standing out because of the global ubiquity, steady upgrading functions and straightforward coupling with optical methods that utilize absorbance/transmittance (Wang et al., 2016a, 2016b; Wei et al., 2014), fluorescence (Tseng et al., 2010; Zhu et al., 2011), chemiluminescence (Zangheri et al., 2015) and spectroscopy of guided waves based on photonic crystal (Gallegos et al., 2013) and surface plasmon resonance (SPR) (Liu et al., 2015; Preechaburana et al., 2012; Wang et al., 2016b). Such developments may provide new solutions for routine daily personal healthcare and tests of contaminants in drinking water and food. It can also serve as a first hand tool for the characterization of injectable biofluids prior to use. Critical reviews on the smartphone biosensors based on optical and electrical detection methods have been reported elsewhere (Roda et al., 2016; Zhang and Liu, 2016).

* Corresponding author.
** Corresponding author at: School of Ophthalmology & Optometry, Eye Hospital, School of Biomedical Engineering, Wenzhou Medical University, Wenzhou 325001, PR China.
E-mail addresses: bliedberg@ntu.edu.sg (B. Liedberg), wangyi@wibe.ac.cn (Y. Wang).

http://dx.doi.org/10.1016/j.bios.2017.07.048
Received 22 April 2017; Received in revised form 15 July 2017; Accepted 18 July 2017
Available online 19 July 2017
0956-5663/

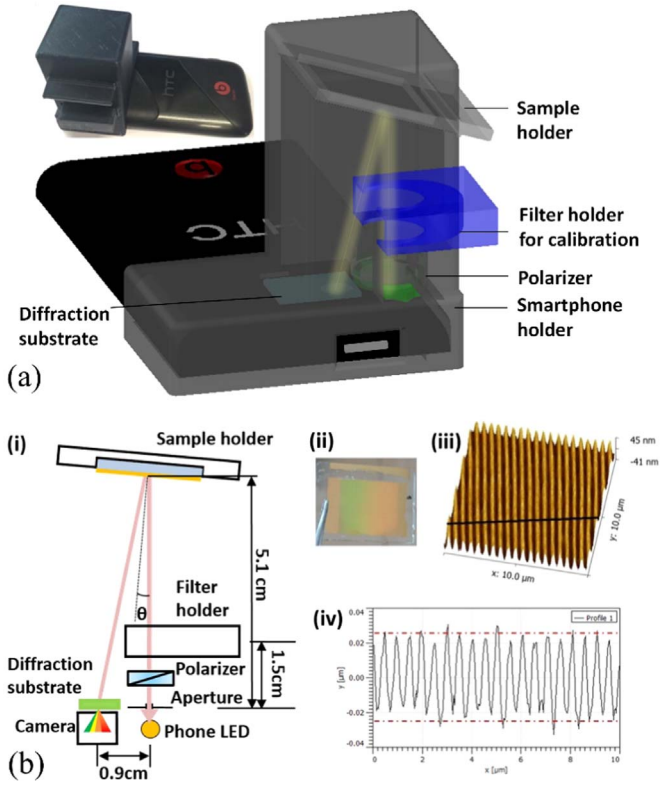

Fig. 1. (a) Schematic structure of the smartphone spectrometer relying the in-built LED light, a CD diffraction substrate and the smartphone camera. Inset is a photo of 3D printing plastic sample chamber kit attached on HTC sensation XE smartphone. (b) The optical arrangement of the smartphone spectrometer (i), and a photo of an Au sensor chip with diffraction grating (ii), a corresponding AFM imaging (iii) and surface profile (iv) of the sensor chip.

Lipopolysaccharide (LPS) also known as endotoxin (Kim et al., 2012) is one of such targets present in the outer membrane of Gram-negative bacteria. It consists of three covalently bound parts, an inner core, outer core and O-antigen. LPS is an inflammatory stimulator that may trigger septic shock. Septic shock is severe pathophysiological syndrome in response to an infection that in many cases is fatal as it can lead to organ failure (Cohen, 2002). Human beings are exposed to LPS through drinking water and injectable biofluids (including various supplements and infusion liquids). The first detection method for LPS, rabbit pyrogen test (RPT) dates back to 1940s (Weary and Wallin, 1973). Other approaches have been established since then including the widely used limulus amoebocyte lysate (LAL) test (Weary et al., 1980). Apart from these complicated methods, some of which involved animals, methods that are fully synthetic and are easy to operate are in great demand.

In this work we demonstrate a portable LPS detection platform based on a smartphone and a grating-coupled SPR (GC-SPR), Fig. 1a. Compared to previous designs of portable biosensors that utilize wavelength interrogation of GC-SPR and immunoassays (Fernandez et al., 2010), the reported sensor system does not require additionally external light source and detector which greatly simplifies the whole platform. In addition, specific analysis of target analyte is assured by using a synthetic peptide receptor immobilized on the sensor chip surface which provides more robust disposable sensor chips with longer shelf-life.

2. Materials and methods

2.1. Materials

Lipopolysaccharides (LPS) from *Klebsiella pneumonia* (L4268) was purchased from Sigma-Aldrich (Singapore). The molecular weight of commercial LPS varies between 4 and 20 kDa. Peptide KC-13 (KKNYSSSISSIHC) and a scrambled peptide YC-13 (YISKSNSSKIHSC) were customized and purchased from GL Biochem (Shanghai, China). UV curable polymer, NOA72 was obtained from Norland (Cranbury, NJ). The plastic sample chamber kit, including a chamber and several sample holders were 3D printed with acrylonitrile butadiene styrene (ABS). Clinical-grade 0.9% sodium chloride intravenous infusion BP was purchased from Hebei Tiancheng Pharmaceutical Co. (Cangzhou, China). Compound sodium lactate intravenous infusion BP was obtained from CR Double-Crane Pharmaceutical Co. (Beijing, China). Insulin aspart were purchased from Novo Nordisk (Bagsvaerd, Denmark). Ethylenediaminetetraacetic acid (EDTA) was obtained from Macklin (Shanghai, China). Other chemicals, including bovine serum albumin (BSA, ca. ~ 66 kDa, ≥ 96%), phosphate-buffered saline (PBS) buffer tablets were purchased from Sigma-Aldrich.

2.2. Preparation of a sensor chip

The Au grating substrate was prepared as reported in our previous work (Wang et al., 2011, 2012). Briefly, a glass substrate was drop casted with UV curable polymer (NOA 72) and a PDMS stamp (replicated from a silicon master) was placed on it and cured under UV light (365 nm) for 2 h. After peeling off the PDMS stamp, the substrate was coated with 2 nm Cr followed by 70 nm Au film.

The grating Au substrates and flat Au film were first cleaned by O_2 plasma for 3 min. After 4 h incubation in aqueous solution with 50 μM KC-13, the surface was rinsed by deionzed water and dried by a stream of N_2. The peptide forms covalent interaction between the Au and thiol terminated group from the cysteine of the peptide. The peptide-modified Au substrates were used further for LPS detection. The flat Au film (2 nm Cr and 47 nm Au coated on glass substrate) were used for conventional prism-coupled SPR measurement.

2.3. Analyte capture on the sensor chip

For characterizing the performance of developed SPR spectrometer, the grating Au substrates were incubated in 1 mg/mL BSA aqueous solution for 20 min. After rinsing with deionzed water, the substrates were dried by a stream of N_2 prior to the measurement of the reflectance color band with the smartphone SPR spectrometer.

For the detection of LPS, the KC-13 modified sensor chips were incubated sequencially with LSP solution with concentrations of 10 ng/mL, 50 ng/mL, 100 ng/mL, 500 ng/mL, 1 μg/mL, 5 μg/mL, and 10 μg/mL. In between the sensor chips were ringsed with water to remove unspecific bond molecules and measured the SPR spectra with the smartphone spectrometer.

2.4. The selectivity test and detection of LPS in clinical matrices

To investigate the selectivity of the sensors, the SPR chips were incubated for 20 min with PBS buffer solution in the presence of 100 μM of glucose, EDTA, citrate, H_3PO_4, acetic acid, glutathione (GSH), ATP and 100 μg/mL BSA, respectively. The SPR dip shifts were recorded after rinsing the sensor chips with PBS buffer, and compared with that measured in PBS buffer in the presence of 100 ng/mL LPS (i.e. 10 nM, provided the molecular weight of 10 kDa).

For the detection of LPS in real samples/matrices, clinical-grade 0.9% sodium chloride intravenous infusion BP, compound sodium lactate intravenous infusion BP, insulin aspart (undiluted and 1 time diluted with PBS) were spiked with 50 ng/mL, 100 ng/mL, 1 μg/mL of LPS. The sensor responses were recorded after 20 min incubation followed by rinsing with PBS buffer. The sensor responses for the same amount of LPS in PBS buffer solution were taken as comparison.

2.5. Calibrating of smartphone spectrometer

To calibrate the smartphone spectrometer, six filters (470 nm ± 20 nm, 482 nm ± 17.5 nm, 525 nm ± 20 nm, 536 nm ± 20 nm, 670 nm ± 20 nm band pass filters, and 550 nm longpass filter) were sequentially placed into the filter holder of the smartphone spectrometer to obtain the spectra and compare it with the one measured with UV–vis spectrometer. The transmission spectra of six filters measured by UV–vis spectrometer were shown in Fig. S1 in the Supporting information. In the smartphone spectrometer, a mirror was inserted into the sample holder and a reference spectrum was obtained without any filters. The filters transmission spectra were accordingly measured by placing the filter into the filter holder (see Fig. 1). Compared with the spectra measured by UV–vis spectrometer, the measurable wavelength range of the smartphone spectrometer was determined as 430–650 nm.

3. Results and discussion

3.1. The development of the smartphone GC-SPR spectrometer

Surface plasmons were excited by a light beam emitted from the smartphone in-built white light LED (HTC sensation XE), which passes through an aperture (0.5 mm) and a polarizer (LPVIS050-MP2, Thorlabs) and impinges under an angle of about θ = 5° at an Au sensor chip with diffraction grating mounted on a sample holder (Fig. 1a). The in-built LED light source covers a wavelength range from 400 to 750 nm, with two strong emission bands located at ~ 450 and ~ 550 nm, respectively (Wang et al., 2016b). The distance between the aperture and the sensor chip surface was set to be 5.1 cm to allow for the light reflect back to the camera. The reflected light passes through a compact disk (CD, with 640 lines/mm) as a transmission diffraction grating to spatially disperse the wavelength spectrum via the first diffraction order which was imaged to the phone CMOS camera (8 Megapixel), see Fig. 1bi. Note that there is a built-in lens on the front of the CMOS sensor to focus the image of the spectrum. In this study, the spectrum image was focused by touching the screen and captured with 4 times of magnification.

3.2. The characterization of GC-SPR sensor chips

The Au grating substrates can be mass produced with the PDMS stamp and UV curing procedure (Fig. 1bii), which is also compatible with roll-to-roll printing. AFM characterization indicated the sinusoidal modulation with period of Λ = 500 nm and modulation depth of d = 50 nm (Fig. 1biii, iv). The GC-SPR on these gratings was firstly analysed by a commercial spectrometer Ocean Optics HR4000 for angles of incidence 0–30° and a grating oriented perpendicular to the plane of incidence, see Fig. 2, and Fig. S2. The GC-SPR associated with the coupling of incident light to surface plasmons via + 1st and − 1st diffraction orders is manifested as a narrow dip in the reflectivity spectrum. The measured spectrum shows that the resonance occurs at normal incidence at around 550 nm. When the angle of incidence is increased, the resonance splits and the − 1st diffraction order branch is red shifted. The −1st order resonant wavelength increases linearly from about 570–730 nm with the incident angle increase from 4° to 25°, as shown in Fig. 2. The coupling to surface plasmons is stronger and the resonant dip is narrower (width of 20–50 nm) for the −1st diffraction order than for the + 1st diffraction order. The reason is that the + 1st diffraction order SPR occurs at short wavelengths close to the plasma frequency of gold. Considering the SPR coupling efficiency and the detectable range of the smartphone spectrometer, the sample holder was therefore designed to provide the incident light of θ = 5° and − 1st diffraction order excitation.

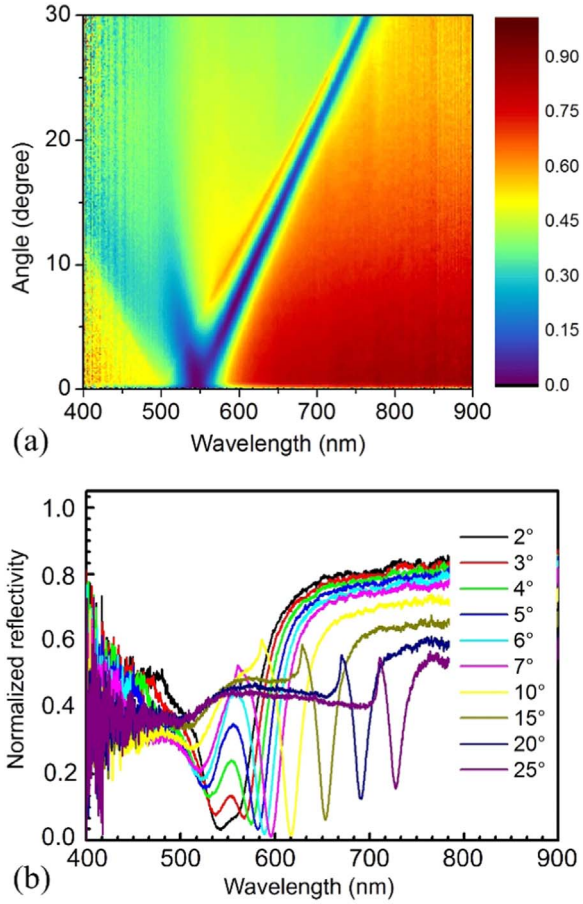

Fig. 2. (a) Measured angular-reflectance dispersion of grating Au substrates under incident angles from 0° to 30° (step of 0.1°) and wavelength range between 400 nm and 900 nm. (b) Reflective spectra of grating Au substrates measured under 10 different incident angles (0°, 3°, 4°, 5°, 6°, 7°, 10°, 15°, 20°, 25°) in air.

3.3. The measurement of the smartphone GC-SPR reflection spectrum

The developed smartphone GC-SPR relies on the measurement of changes in the wavelength reflectivity spectrum. Dispersed wavelength spectrum was imaged to the smartphone CMOS detector at area of about 900 pixels × 50 pixels. Five spectra were accumulated to decrease the noise. As seen in Fig. 3a, the acquired image from CMOS camera shows a bright stripe with wavelength-dispersed light intensity that was reflected from the sensor chip. In order to convert the pixels along the stripe to wavelength λ, the optical arrangement was calibrated by using a mirror and a set of known transmission filters. The GC-SPR spectrum was obtained by averaging the intensity perpendicular to stripe yielding a raw spectrum I(λ). The raw spectrum measured for the sensor chip $I_s(\lambda)$ was normalized with that obtained for a reference mirror $I_0(\lambda)$ in order to obtain reflectivity $R(\lambda) = I_s(\lambda)/I_0(\lambda)$. The spectra were then proceed by Savitzky-Golay method with 30 points of window and polynomial order of 5.

In order to demonstrate the sensitivity of developed smartphone SPR spectrometer to refractive index changes on the sensor chip surface, BSA monolayer was physisorbed on the gold surface. The rainbow stripe shows a dark band corresponding to the SPR resonant band which shifts to higher wavelength after the adsorption of BSA (marked in red arrow in Fig. 3a). The − 1st order excitation of surface plasmons on gold surface is manifested as a narrow dip in the reflectivity spectrum centered at 581 nm (Fig. 3b). After the surface was coated with BSA monolayer, the SPR wavelength shifts to about 589 nm. Therefore, due to the high sensitivity of SPR to refractive index changes, such a smartphone SPR spectrometer shows the feasibility for biomolecule detection.

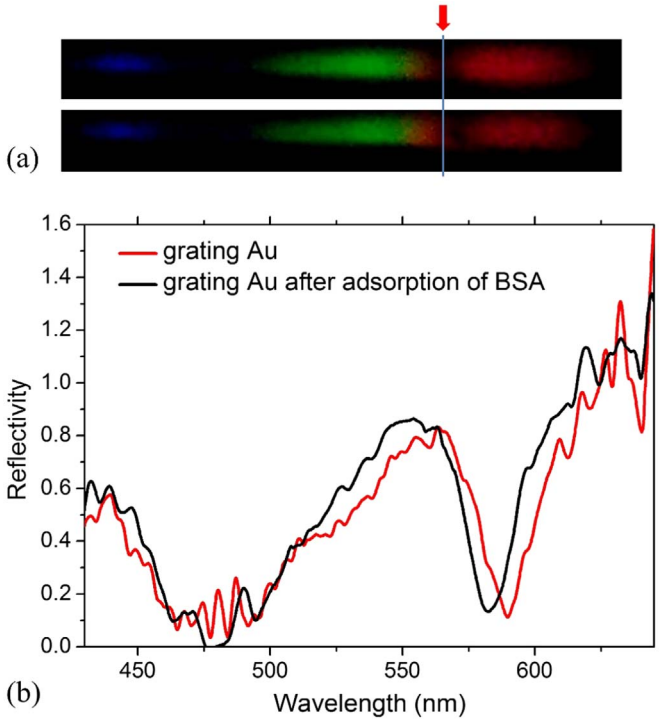

Fig. 3. (a) Color bands of grating Au before (upper one) and after incubation with 1 mg/mL BSA, measured under incident angle of 5°. The line and red arrow indicate the SPR dip on the color band. (b) The corresponding SPR spectra of grating Au substrate before (black curve) and after (red curve) non-specific binding of BSA. (For interpretation of the references to color in this figure legend, the reader is referred to the web version of this article.)

3.4. The detection of LPS with smartphone SPR spectrometer

We accordingly modified the grating Au substrate with a synthetic peptide receptor for specific detection of LPS (from *Klebsiella pneumonia*) based on the smartphone SPR spectrometer. Peptide-functionalized metallic surface (nanostructures) has been widely applied in our group for sensing applications including the detection of toxins (Liu et al., 2014b; Wang et al., 2014), ions and protein biomarkers (Aili et al., 2009; Chen et al., 2013; Zhang et al., 2015). In this smartphone SPR spectrometer, we modified the grating Au substrate with KC-13 peptide (KKNYSSSISSIHC). The synthetic peptide shows high affinity to the binding of LPS as reported previously (Lim et al., 2015; Suzuki et al., 2010). After incubation of the KC-13 modified sensor chip with concentrations of LPS in water between 10 ng/mL and 10 μg/mL for 20 min, the SPR spectra were measured by using the smartphone spectrometer. As shown in the rainbow stripe changes on different concentration of LPS (Fig. 4a), red shifts on the dark band were observed. Accordingly, the SPR reflectivity spectra show the resonant wavelength shifts to higher wavelength upon increasing the concentration of LSP applied on the sensor chip. The resonant wavelength shift of 1.46 nm was observed upon the incubation of 10 ng/mL LPS on the sensor surface, and wavelength shifts up to 5.66 nm at presence of 10 μg/mL LPS (Fig. 4b). The signal-to-noise ratio for 1 μg/mL LPS is about 2.4 (Fig. 4c) which is about 3.6-fold lower than that measured with conventional prism-coupled SPR setup (see Fig. S3 in the Supporting information). This is due to the higher noise of smartphone SPR spectrometer and the chip-to-chip variations. Note that the signal-to-noise ratio is computed based on the signal divided by 3 times of the standard deviation (3 × SD = 2.1 nm) of SPR dip wavelength for 5 different chips. The calibration curve based on monitoring the resonant wavelength shift indicated that the limit of detection (LOD) for the detection of LPS down to 32.5 ng/mL can be achieved with the smartphone SPR spectrometer (Fig. 4c). The LOD was determined as

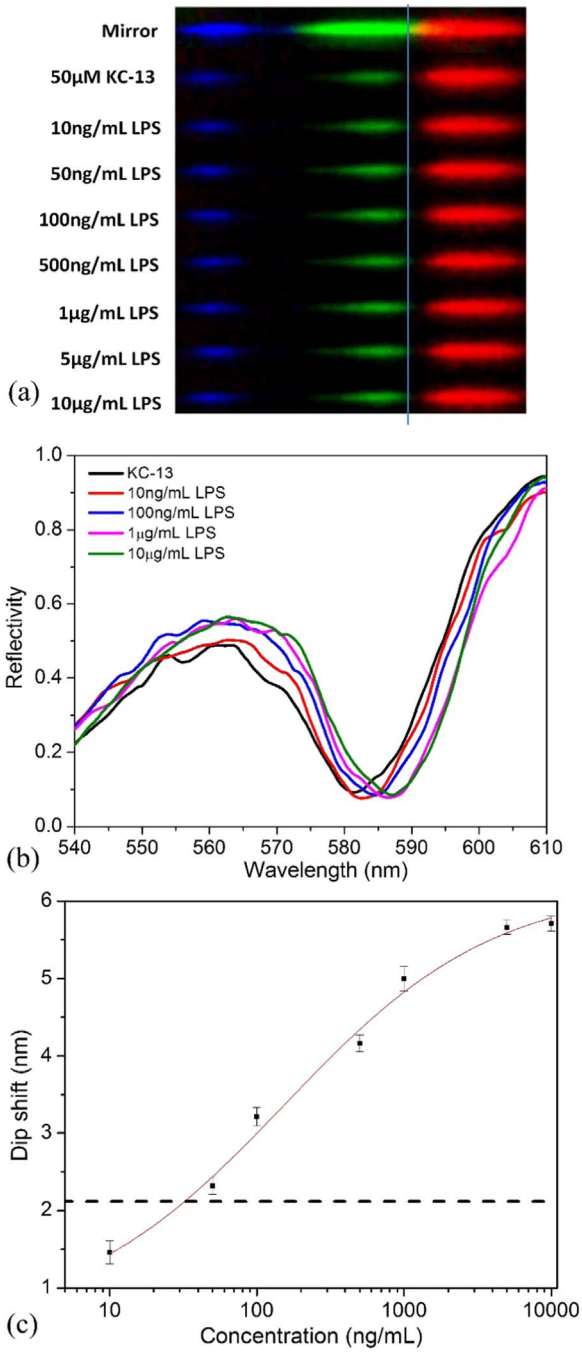

Fig. 4. (a) Color bands measured on mirror as a reference and peptide-modified grating Au substrate after incubation with various concentration of LPS from 0 to 10 μg/mL. The line indicates the SPR resonant band changes. (b) The corresponding spectra of grating Au substrate after incubation with different concentration of LPS. (c) The sigmoidal fitted calibration curve (red) with the noise level (dashed black curve) estimated as 3 times of standard deviation of SPR dip wavelength on 5 different chips. (For interpretation of the references to color in this figure legend, the reader is referred to the web version of this article.)

the concentration of LPS at which the response is 3 times of the standard deviation (3 × SD = 2.1 nm) of dip wavelength measured with 5 different chips. The high noise could be mainly ascribed to the variation for the chips fabrication/modification. Note that the error bars were obtained from measurements of 3 different chips. Our method has shown at least 10-fold lower LOD as compared with fluorescence based LPS detection (~ 1.5 μg/mL) (Voss et al., 2007), fluorescence turn-on detection (280 ng/mL) (Liu et al., 2014a), and other methods (Wu et al., 2011).

In addition, the selectivity of the sensor was investigated by incubating sensor chips with various small or macro-biomolecules, such as 100 μM of glucose, EDTA, phosphate, citrate, ATP, GSH, acetic acid and 100 μg/mL of BSA in PBS buffer solution. The SPR responses were compared with that measured in 100 ng/mL LPS in PBS (Fig. S4 in the Supporting information). The results show that the response for most of the tested analytes are comparable with the blank samples, about 5-fold lower dip shifts as compared with that of 100 ng/mL LPS. For 100 μg/mL of BSA (1000-fold higher than LPS concentration), it shows a relative higher response (about 3-fold lower than that of LPS response) due to the nonspecific adsorption of BSA on the chip surface. Overall, the sensor chips show good selectivity for the detection of LPS. Note that the sensor as measured for the detection of LPS at concentration from 50 ng/mL to 1 μg/mL in PBS (Fig. S4 in the Supporting information) provides about 10% higher response as that measured in water (Fig. 4c). It might be ascribed to the higher ionic strength in PBS which improved the LPS interactions with KC-13. In addition, a control experiment was also carried out on the scrambled peptide (YC-13) modified sensor chip for the study of the nonspecific binding of LPS. The results show that the response for the nonspecific binding of 100 ng/mL LPS was comparable with the blank sample (Fig. S4 in the Supporting information).

For the real samples/matrices detection, we tested our sensor with three injectable clinical solutions, which require a reliable and sensitive endotoxin test to ensure the absence of LPS before being injected into a patient. The injectable solutions, i.e. clinical-grade 0.9% sodium chloride intravenous infusion, compound sodium lactate intravenous infusion and insulin aspart (undiluted and 1 time diluted with PBS) were spiked with LPS at final concentrations of 50 ng/mL, 100 ng/mL and 1 μg/mL. The response for the LSP-spiked sodium chloride and compound sodium lactate matrices (simple infusion solution but may contain unknown additives such as stabilizer that interferes with LPS) shows comparable response as in PBS buffer (Fig. S5 in the Supporting information). However, the insulin sample is more complicated, which shows significant reduce of sensor response due to the inhibition of insulin itself or additives in the sample solution. This inhibition effect can be reduced by 1 time dilution of the insulin aspart with PBS buffer, as indicated in Fig. S5. The reproducibility test was also carried out over 10 different chips on the measurement of 100 ng/mL LPS in clinical-grade sodium chloride intravenous infusion, and the results show the response deviation of SD = 0.21 nm. Note that the response was recorded from the SPR dip shift on the same chip before and after incubation with the LPS-spiked solution. Therefore, we believe this method is applicable for the detection of LPS in commonly used infusion solutions. We expect that this small, low-cost smartphone SPR spectrometer can be generally applied for point-of-care diagnosis, food safety control and environment monitoring in near future.

4. Conclusions

In summary, we have built a grating-coupled SPR smartphone spectrometer and applied it for the detection of lipopolysaccharides (LPS). This optical instrument does not contain electronic components and solely relies on the LED flash light source and the CMOS camera built in the used smartphone. The spectrometer is able to perform the analysis in a spectral range of 430–650 nm and it was employed for SPR spectroscopy on sensor chips with Au diffraction gratings that are be prepared by mass production-compatible means. As a receptor, synthetic peptide KC-13 ligand was immobilized on the Au grating sensor chip for specific capture of LPS. The measurement was performed *ex situ* based on monitoring the resonant wavelength shift. The results show the feasibility for the detection of LPS at detection limit of 32.5 ng/mL, and good selectivity for the LSP detection with practical application for real samples/matrices detection such as clinical injectable fluids. We expect that the small and low-cost smartphone SPR spectrometer will be widely applied in field detection in near future.

Acknowledgement

The authors thank for the financial support from the National Natural Science Foundation of China (21605116), Public Projects of Zhejiang Province (2017C33193), Public Projects of Wenzhou (Y20160065, Y20160067), Wenzhou Government's Startup Fund (WIBEZD2014004-02) and Science & Engineering Research Council (SERC) of Agency for Science, Technology and Research (A*STAR), Singapore, for projects under the numbers of 102 152 0014 and 102 152 0015. IK acknowledges support from the Austrian Science Fund (FWF) through the project TRP 304-N20 PLASMOSOL.

Appendix A. Supporting information

Supplementary data associated with this article can be found in the online version at doi:10.1016/j.bios.2017.07.048.

References

Aili, D., Selegard, R., Baltzer, L., Enander, K., Liedberg, B., 2009. Colorimetric protein sensing by controlled assembly of gold nanoparticles functionalized with synthetic receptors. Small 5 (21), 2445–2452.
Chen, P., Selegard, R., Aili, D., Liedberg, B., 2013. Peptide functionalized gold nanoparticles for colorimetric detection of matrilysin (MMP-7) activity. Nanoscale 5 (19), 8973–8976.
Cohen, J., 2002. The immunopathogenesis of sepsis. Nature 420 (6917), 885–891.
Fernandez, F., Hegnerova, K., Piliarik, M., Sanchez-Baeza, F., Homola, J., Marco, M.P., 2010. A label-free and portable multichannel surface plasmon resonance immunosensor for on site analysis of antibiotics in milk samples. Biosens. Bioelectron. 26 (4), 1231–1238.
Gallegos, D., Long, K.D., Yu, H., Clark, P.P., Lin, Y., George, S., Nath, P., Cunningham, B.T., 2013. Label-free biodetection using a smartphone. Lab Chip 13 (11), 2124–2132.
Hay Burgess, D.C., Wasserman, J., Dahl, C.A., 2006. Global health diagnostics. Nature 444 (S1), 1–2.
Kim, S.-E., Su, W., Cho, M., Lee, Y., Choe, W.-S., 2012. Harnessing aptamers for electrochemical detection of endotoxin. Anal. Biochem. 424 (1), 12–20.
Lim, S.H., Feng, L., Kemling, J.W., Musto, C.J., Suslick, K.S., 2009. An optoelectronic nose for the detection of toxic gases. Nat. Chem. 1 (7), 562–567.
Lim, S.K., Chen, P., Lee, F.L., Moochhala, S., Liedberg, B., 2015. Peptide-assembled graphene oxide as a fluorescent turn-on sensor for lipopolysaccharide (Endotoxin) detection. Anal. Chem. 87 (18), 9408–9412.
Liu, F., Mu, J., Wu, X., Bhattacharjya, S., Yeow, E.K., Xing, B., 2014a. Peptide-perylene diimide functionalized magnetic nano-platforms for fluorescence turn-on detection and clearance of bacterial lipopolysaccharides. Chem. Commun. 50 (47), 6200–6203.
Liu, X., Wang, Y., Chen, P., Wang, Y., Zhang, J., Aili, D., Liedberg, B., 2014b. Biofunctionalized gold nanoparticles for colorimetric sensing of botulinum neurotoxin A light chain. Anal. Chem. 86 (5), 2345–2352.
Liu, Y., Liu, Q., Chen, S., Cheng, F., Wang, H., Peng, W., 2015. Surface plasmon resonance biosensor based on smart phone platforms. Sci. Rep. 5, 12864.
Mudanyali, O., Dimitrov, S., Sikora, U., Padmanabhan, S., Navruz, I., Ozcan, A., 2012. Integrated rapid-diagnostic-test reader platform on a cellphone. Lab Chip 12 (15), 2678–2686.
Potyrailo, R.A., Burns, A., Surman, C., Lee, D.J., McGinniss, E., 2012. Multivariable passive RFID vapor sensors: roll-to-roll fabrication on a flexible substrate. Analyst 137 (12), 2777–2781.
Preechaburana, P., Gonzalez, M.C., Suska, A., Filippini, D., 2012. Surface plasmon resonance chemical sensing on cell phones. Angew. Chem. Int. Ed. 51 (46), 11585–11588.
Rakow, N.A., Suslick, K.S., 2000. A colorimetric sensor array for odour visualization. Nature 406 (6797), 710–713.
Roda, A., Michelini, E., Zangheri, M., Di Fusco, M., Calabria, D., Simoni, P., 2016. Smartphone-based biosensors: a critical review and perspectives. TrAC-Trend Anal. Chem. 79, 317–325.
Shen, L., Hagen, J.A., Papautsky, I., 2012. Point-of-care colorimetric detection with a smartphone. Lab Chip 12 (21), 4240–4243.
Suzuki, M.M., Matsumoto, M., Yamamoto, A., Ochiai, M., Horiuchi, Y., Niwa, M., Omi, H., Kobayashi, T., Takagi, T., 2010. Molecular design of LPS-binding peptides. J. Microbiol. Methods 83 (2), 153–155.
Tseng, D., Mudanyali, O., Oztoprak, C., Isikman, S.O., Sencan, I., Yaglidere, O., Ozcan, A., 2010. Lensfree microscopy on a cellphone. Lab Chip 10 (14), 1787–1792.
Voss, S., Fischer, R., Jung, G., Wiesmuller, K.H., Brock, R., 2007. A fluorescence-based synthetic LPS sensor. J. Am. Chem. Soc. 129 (3), 554–561.
Wang, L.-J., Sun, R., Vasile, T., Chang, Y.-C., Li, L., 2016a. High-throughput optical sensing immunoassays on smartphone. Anal. Chem. 88 (16), 8302–8308.
Wang, S., Xu, F., Demirci, U., 2010a. Advances in developing HIV-1 viral load assays for resource-limited settings. Biotechnol. Adv. 28 (6), 770–781.
Wang, W., Wu, W.-Y., Wang, W., Zhu, J.-J., 2010b. Tree-shaped paper strip for semiquantitative colorimetric detection of protein with self-calibration. J.

Chromatogr. A 1217 (24), 3896–3899.
Wang, Y., Dostalek, J., Knoll, W., 2011. Magnetic nanoparticle-enhanced biosensor based on grating-coupled surface plasmon resonance. Anal. Chem. 83 (16), 6202–6207.
Wang, Y., Knoll, W., Dostalek, J., 2012. Bacterial pathogen surface plasmon resonance biosensor advanced by long range surface plasmons and magnetic nanoparticle assays. Anal. Chem. 84 (19), 8345–8350.
Wang, Y., Liu, X., Chen, P., Tran, N.T., Zhang, J., Chia, W.S., Boujday, S., Liedberg, B., 2016b. Smartphone spectrometer for colorimetric biosensing. Analyst 141 (11), 3233–3238.
Wang, Y., Liu, X., Zhang, J., Aili, D., Liedberg, B., 2014. Time-resolved botulinum neurotoxin A activity monitored using peptide-functionalized Au nanoparticle energy transfer sensors. Chem. Sci. 5 (7), 2651–2656.
Weary, M.E., Donohue, G., Pearson, F.C., Story, K., 1980. Relative potencies of four reference endotoxin standards as measured by the limulus amoebocyte lysate and USP rabbit pyrogen tests. Appl. Environ. Microbiol. 40 (6), 1148–1151.
Weary, M.E., Wallin, R.F., 1973. The rabbit pyrogen test. Lab. Anim. Sci. 23 (5), 677–681.
Wei, Q.S., Nagi, R., Sadeghi, K., Feng, S., Yan, E., Ki, S.J., Caire, R., Tseng, D., Ozcan, A., 2014. Detection and spatial mapping of mercury contamination in water samples using a smart-phone. ACS Nano 8 (2), 1121–1129.
Wu, J., Zawistowski, A., Ehrmann, M., Yi, T., Schmuck, C., 2011. Peptide functionalized polydiacetylene liposomes act as a fluorescent turn-on sensor for bacterial lipopolysaccharide. J. Am. Chem. Soc. 133 (25), 9720–9723.
Zangheri, M., Cevenini, L., Anfossi, L., Baggiani, C., Simoni, P., Di Nardo, F., Roda, A., 2015. A simple and compact smartphone accessory for quantitative chemiluminescence-based lateral flow immunoassay for salivary cortisol detection. Biosens. Bioelectron. 64, 63–68.
Zhang, D., Liu, Q., 2016. Biosensors and bioelectronics on smartphone for portable biochemical detection. Biosens. Bioelectron. 75, 273–284.
Zhang, J., Wang, Y., Wong, T.I., Liu, X., Zhou, X., Liedberg, B., 2015. Electrofocusing-enhanced localized surface plasmon resonance biosensors. Nanoscale 7 (41), 17244–17248.
Zhu, H., Yaglidere, O., Su, T.-W., Tseng, D., Ozcan, A., 2011. Cost-effective and compact wide-field fluorescent imaging on a cell-phone. Lab Chip 11 (2), 315–322.